Optik - International Journal for Light and Electron Optics 170 (2018) 506–511

Contents lists available at ScienceDirect

Optik

journal homepage: www.elsevier.com/locate/ijleo

Original research article

Directional gated imaging in a turbid medium using an ultrafast optical Kerr gate

Yuhu Ren[a], Wenjiang Tan[a,*], Yipeng Zheng[a], Xiaojing Liu[a], Junyi Tong[b]

[a] Key Laboratory for Physical Electronics and Devices of the Ministry of Education & Shaanxi Key Lab of Information Photonic Technique, School of Electronics & information Engineering, Xi'an Jiaotong University, Xianning-xilu 28, Xi'an, 710049, China
[b] Departments of Applied Physics, Xi'an University of Technology, Xi'an, 710048, China

ARTICLE INFO

Keywords:
Directional filter
Ballistic imaging
Optical Kerr effect
Turbid medium
Cylindrical lens

ABSTRACT

Directional gated imaging of hidden objects in scattering media is demonstrated using an ultrafast optical Kerr gate (OKG), in which the gating and imaging beams are focused by utilizing a cylindrical lens and a convergent lens, respectively. Owing to the spatial transmission characteristics of the directional gate, a rectangular aperture stop is formed, which leads to different resolution limits for vertical and horizontal structures of an object. By implementing directional gated imaging, the directional feature can be extracted from an original image.

1. Introduction

Oriented linear or piecewise linear patterns are common phenomena in nature, which forms an important class of images [1]. An effective technique for extracting the directional feature from an original image is based on Fourier transform analysis because it enables the separation of their different spatial frequencies. Directional filters in the Fourier domain are used in different applications, such as image coding [2], design of fan filters [3], and texture discrimination [4]. Many directional filters are also used for digital image processing to extract the directional feature from an original image [5–7]. Compared to the directional filter used by the digital imaging processing method, a full optical directional filter enables immediate processing. Notable examples of the optical directional filters used by the optical Fourier transform have been used for defecting detects in textured materials [8,9].However, most studies on extracting the directional feature from an original image were conducted in a non-scattering environment.

Optical imaging of targets embedded in highly scattering media, such as biological tissues [10–13], fog [14], or diesel sprays [15,16] is a challenging problem because multiple scattering of light by the turbid media scramble optical information for imaging. Moreover, the image quality is often degraded because of the noise that arises from the multiple scattering in a scattering medium. Light transmitted through a turbid medium comprises ballistic, snake, and diffuse components [17]. The difference in the transit time can be exploited to sense objects [18,19] hidden in a scattering medium by detecting only the ballistic component but excluding delayed scattered photons. Among available time gating techniques, optical Kerr gate (OKG) has been investigated widely because of its advantages, such as no need for the satisfaction of the phase-matching condition or the capability to acquire a time-sliced true 2D spatial image for both incoherent and coherent optical signals [20–24]. However, most studies on OKG imaging give little information on the directional feature from imaging of hidden objects in a scattering medium. For example, liquid/gas interfaces in a high-pressure spray cannot be clearly seen only using OKG imaging without a digital image post-processing algorithm [25]. Therefore, the development of a directional gated imaging system which is an all-optical system is helpful for extracting gas/fuel jet interfaces in sprays.

* Corresponding author.
E-mail address: tanwenjiang@mail.xjtu.edu.cn (W. Tan).

https://doi.org/10.1016/j.ijleo.2018.05.139
Received 20 April 2018; Received in revised form 21 May 2018; Accepted 31 May 2018

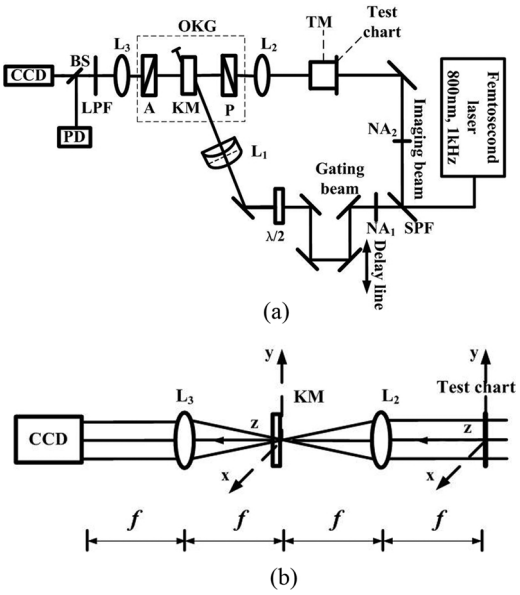

Fig. 1. (a) Experimental setup of the directional gated imaging system. (b) Schematic of the 4*f* imaging system. L_1: cylindrical lens; L_2, and L_3: lenses; SPF: short pass filter; λ/2: half-wave plate; P: polarizer; A: analyzer; NA: neutral attenuator; LPF: long pass filter; TM: turbid medium; KM: Kerr medium; BS: beam splitter; OKG: optical Kerr gate; and f: focal length of lenses L_2, and L_3.

In this paper, we demonstrate a directional gated imaging through a turbid medium by use of an ultrafast OKG, in which the gating and imaging beams are focused by utilizing a cylindrical lens and a convergent lens, respectively. A sequence of directional gated images of a test chart hidden behind a highly turbid medium was obtained by means of the directional filter technique. Owing to the spatial transmission characteristics of the directional gate, a rectangular aperture stop was formed, which led to different resolution limits for vertical and horizontal structures of an object. Using directional gated imaging, the directional feature of an original image can be extracted and the contrast of directional gated images can be enhanced significantly.

2. Experimental setup

The schematic of the directional gated imaging system is shown in Fig. 1 (a). A Ti:sapphire laser was used to provide light pulses with a central wavelength of 800 nm, full width at half maximum of 50 *f*s, and repetition rate of 1 kHz. The laser beam was split into a gating beam centered at 780 nm and an imaging beam centered at 800 nm by a short pass filter (SPF). The intensities of the gating and imaging beams were adjusted by neutral attenuators NA_1 and NA_2, respectively. The imaging beam was first modulated by a 1.41-line-pair/mm resolution chart (a chromium-coated glass U.S. Air Force resolution chart) and then introduced to a turbid medium. The transmitted light from the turbid medium was first focused by lens L_2 and then introduced into the OKG. The OKG consists of a pair of crossed polarizers and a CS_2 cell. The gating beam was first linearly polarized at 45° with respect to the polarization of the imaging beam for the optimal efficiency using a half-wave (λ/2) plate. The gating beam was focused by cylindrical lens L_1 with focal length f_1 = 150 mm into the Kerr medium of CS_2 filled in a quartz cell of thickness 5 mm. This is the main difference from the conventional OKG [26–30], in which the gating beam is focused by a convergent lens. The cylindrical lens is used to adjust the shape of the gating beam. The magnification of circular light by a cylindrical lens can be different for two perpendicular directions [31].

The cylindrical lens L_1 was used to change circular light into rectangular light. Convergent Lenses L_2 and L_3 both with focal lengths f = 150 mm formed a 4*f* imaging system as shown in Fig. 1 (b). In this imaging system, the imaging pulse was spatially overlapped with the gating pulse in the Kerr medium which was placed at the back focal plane (Fourier-transform spectrum plane) of lens L_2. When the two pulses were spatially and temporally overlapped, the imaging pulse polarization was rotated owing to the birefringence of the Kerr media induced by the gating pulse. Then a part of the imaging pulse passed through an analyzer, which was synchronously detected by a charge coupled device (CCD) camera and a photodiode (PD).

The turbid medium was composed of a polystyrene microsphere solution contained in a cubic cuvette with inside dimensions of 50 mm × 50 mm × 10 mm. The cuvette thickness along the optical axis was 10 mm. The diameter of the polystyrene microsphere was 3.13 μm. The refractive indices of the background medium n_b and the polystyrene microspheres n_p were 1.33 and 1.58, respectively. The absorption of the turbid medium was low enough to be neglected. The value of the optical depth (OD) of the sample was 9.9.

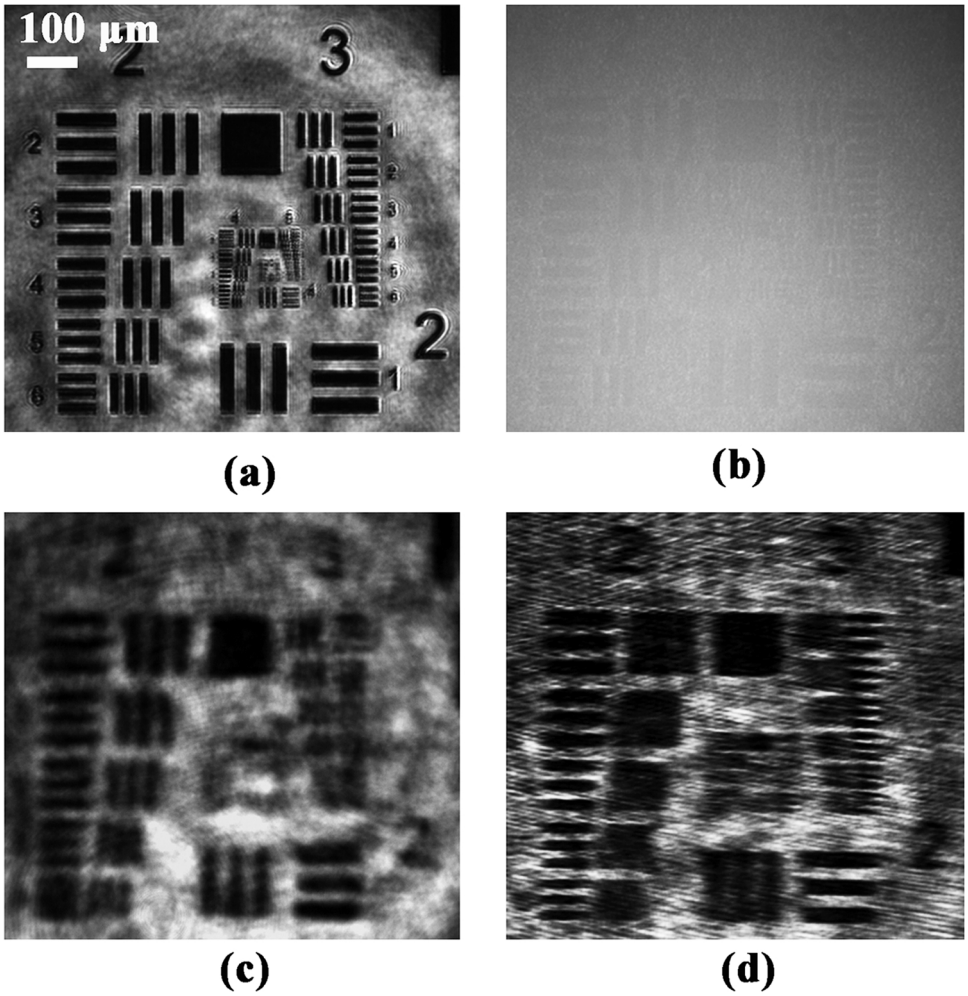

Fig. 2. Images of the test chart behind water and the polystyrene microsphere turbid medium. (a) Reference image. (b) No time gate (standard transillumination). (c) Conventional OKG imaging. (d) Horizontal patterns of the object selected by the directional gate.

3. Results and discussions

The images of the test chart (U.S. Air Force 1951 resolution chart) hidden behind a polystyrene microsphere sample are demonstrated using directional gated imaging. In Fig. 2(a), we show the direct images of the sample filled with deionized water as the reference image. In Fig. 2(b), we show the direct images of the sample filled with the polystyrene microsphere turbid medium. In Fig. 2(c) and (d), we show the conventional OKG and directional gated images of the polystyrene microsphere turbid medium, respectively. As shown in Fig. 2(b), an object hidden behind such a turbid medium cannot be seen owing to a great number of scattered photons. In Fig. 2(c), the bars in Group 3 of the target are highly blurred although the conventional OKG can select full features of the imaged object. In Fig. 2(d), only the horizontal patterns of the imaged object can be seen clearly for the directional gated imaging in the turbid medium. Hence, using directional gated imaging, the directional feature of an original image can be extracted.

The reason for the difference between conventional OKG imaging and directional gated imaging can be explained as follows. The OKG and directional gate act as different type of spatial filters because they can select different spatial frequency components of the object. The OKG acts as a 2D circular Gaussian filter and the directional gate acts as a 1D Gaussian filter. The spatial filters are performed by the transient soft apertures in the Kerr material, which originate from the finite spot size of the gating beams. In the experimental setup, the optical Fourier transform of the object is performed in the focal plane of lens L_2, where different spatial frequencies belonging to the examined structure are shown separately. For the conventional OKG, the transient soft circular aperture enables the low-spatial frequency components of the imaged object pass but removes the high-spatial frequency components. The low-spatial frequency components are at the center of the Fourier plane of the lens (L_2), while the high-spatial frequency components are in the peripheral area of the Fourier plane. For the directional gate, the transient soft rectangular aperture enables the vertical spatial frequency components of the imaged object pass but removes the horizontal spatial frequency components. Because the bar

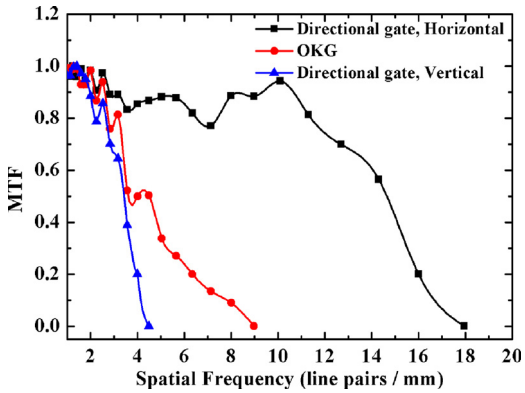

Fig. 3. Comparison of the contrast of the conventional OKG and directional gated images.

length in the test chart is longer than that bar width, the vertical spatial frequency components are mainly at the horizontal direction of the Fourier plane of the lens (L_2). The results show that the directional gated imaging can effectively select the directional features from the original image and simultaneously remove scattered photons.

To quantitatively evaluate the performance of the OKG and directional gated imaging systems, we measured the modulation transfer function (MTF) of both systems. The MTF is given by $MTF(f) = C(f)/C_0(f)$, where the image contrast is defined as $C(f) = (I_{max} - I_{min})/(I_{max} + I_{min})$, Further, $C_0(f)$ denotes the modulation of the object and f is the spatial frequency. The image contrast is calculated using the average light intensity retrieved from the dark region (I_{min}) and the average light retrieved from the unshadowed region (I_{max}) of the test chart. In Fig. 3, the MTF was evaluated for the horizontal and vertical lines. For the directional gated imaging, there is a distinct difference for both directions. At high-spatial frequencies, the contrast of the vertical lines is clearly lower than that of the horizontal lines. This difference is caused by the 1D Gaussian filter originating from the linearly gating beam. For the horizontal lines, the maximum resolvable spatial frequency is 17.95 l in. pairs per millimeter (lp/mm), and the corresponding resolved object size is approximately 27.84 μm in our experiments. For the vertical lines, the maximum resolvable spatial frequency is 4.49 lp/mm, and the corresponding resolved object size is approximately 111.36 μm in our experiments. However, for the conventional OKG imaging system the maximum resolvable spatial frequency for both directions is 8.98 lp/mm, and the corresponding resolved object size is approximately 55.7 μm. The results show that directional gated imaging can effectively exact the directional feature from an original image and increase the horizontal resolution at the expense of the vertical resolution. In addition, the horizontal contrast of directional gated imaging can also be enhanced. The reason for the increase of the horizontal resolution at the expense of the vertical resolution can be explain as follows. In this experiment, the intensity of the gating beam remain unchanged. The collimated gating beam is expanded in the vertical direction and narrowed in the horizontal direction using the cylindrical lens, which leads to the horizontal high spatial frequency components of the directional feature filtered by the conventional OKG can be compensated using the directional gate. It should be noted that the same results can also be obtained by performing Fourier transformation using the obtained images. However, the digital imaging processing method cannot exact the directional feature of images in real time.

As one of the potential applications, we finally performed an experiment to image an object behind a turbid medium using the directional gate. The object was fabricated in glass using a femtosecond laser, which resembled “LITTLE.” In Fig. 4(a), we show the direct image of the sample filled with the polystyrene microsphere turbid medium. The object hidden behind such a turbid medium cannot be recognized. In Fig. 4(b), we show the direct image of the sample filled with deionized water as the reference image. In Fig. 4(c) and (d), we show different directional gated images of the polystyrene microsphere turbid medium. As shown in Fig. 4(c), only the vertical patterns are selected by the directional gate in the turbid medium. Likely, as shown in Fig. 4(d), only the horizontal patterns are selected by the directional gate in the turbid medium. These results show that the directional gated imaging technique can be used to extract the directional features of objects hidden in turbid media.

4. Conclusions

In summary, we demonstrated directional gated imaging through a turbid medium using an OKG, in which, the gating and imaging beams were focused by implementing a cylindrical lens and a lens, respectively. A sequence of directional gated images of a test chart hidden behind a highly turbid medium was obtained through the directional filter technique. The results show that the directional features can be extracted from an original image by selecting a part of the spatial frequency components. In addition, the contrast of directional gated images can be enhanced significantly. The directional gated imaging technique is potentially applicable to directional feature extraction from an original image hidden in highly scattering media, such as fiber orientation in the inner arterial media.

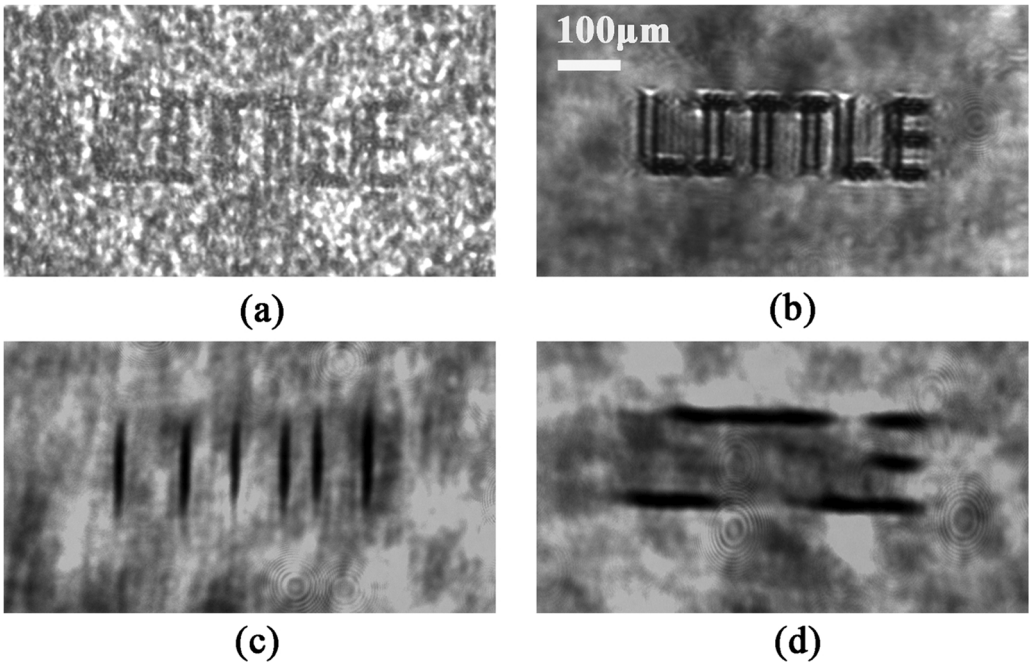

Fig. 4. Images of the object fabricated in a glass hidden behind the water and the polystyrene microsphere turbid medium. (a) No time gate (standard transillumination). (b) Reference image. (c) Vertical patterns of the imaged object selected by the directional gate. (d) Horizontal patterns of the object selected by the directional gate.

Acknowledgements

The authors gratefully acknowledge the financial support for this work provided by the National Natural Science Foundation of China under the Grant Nos. 61427816, 61235003, 61205129 and 61308036; the Natural Science Basic Research Plan in Shaanxi Province of China (Program No. 2014JQ8363); the Open Found of State Key Laboratory on Integrated Optoelectronics (IOSKL2015KF24). This work was also supported by Collaborative Innovation Center of Suzhou Nano Science and Technology.

References

[1] L.H. Timmins, Q.F. Wu, A.T. Yeh, J.E. Moore Jr., S.E. Greenwald, Structural inhomogeneity and fiber orientation in the inner arterial media, Am. J. Physiol. Heart Circ. Physiol. 298 (2010) H1537–H1545.
[2] X.L. Peng, J.Z. Xu, Highly parallel line-based image coding for many cores, IEEE Trans. Image Process. 21 (2012) 196–206.
[3] T. Sekiguchi, Y. Karasawa, Wideband beamspace adaptive array utilizing FIR fan filters for multibeam forming, IEEE Trans. Signal. Proces. 48 (2000) 278–284.
[4] T. Ahonen, M. Pietikäinen, Image description using joint distribution of filter bank responses, pattern recogn. Lett. 30 (2009) 368–376.
[5] G. Swamy, K. Balasubramaniam, Directional filter bank-based segmentation for improved evaluation of nondestructive evaluation images, NDT & E Int. 40 (2007) 250–257.
[6] W.R. Boukabou, A. Bouridane, S. Al-Maadeed, Enhancing face recognition using directional filter banks, Digit. Signal Process. 23 (2013) 586–594.
[7] M. Habib, A. Hussain, T. Choi, Adaptive threshold based fuzzy directional filter design using background information, Appl. Soft. Comput. 29 (2015) 471–478.
[8] C. Ciamberlini, F. Francini, G. Longobardi, P. Sansoni, B. Tiribilli, Defect detection in textured materials by optical filtering with structured detectors and self-adaptable masks, Opt. Eng. 35 (1996) 838–844.
[9] J. Molleda, R. Usamentiaga, D.F. Garcia, F.G. Bulnes, A. Espina, B. Dieye, L.N. Smith, An improved 3D imaging system for dimensional quality inspection of rolled products in the metal industry, Comput. Ind. 64 (2013) 1186–1200.
[10] E. Edrei, G. Scarcelli, Optical imaging through dynamic turbid media using the fourier-domain shower-curtain effect, Optica 3 (2016) 71–74.
[11] Z.B. Xu, J.J. Liu, D.H. Hong, V.Q. Nguyen, M.R. Kim, S.I. Mohammed, Y.L. Kim, Back- directional gated spectroscopic imaging for diffuse light suppression in high anisotropic media and its preclinical applications for microvascular imaging, IEEE J. Sel. Top. Quant. 16 (2010) 815–823.
[12] H. Yu, J. Park, K.R. Lee, J. Yoon, K.D. Kim, S. Lee, Y.K. Park, Recent advances in wavefront shaping techniques for biomedical applications, Curr. Appl. Phys. 15 (2015) 632–641.
[13] A.P. Mosk, A. Lagenddijk, G. Lerosey, M. Fink, Controlling waves in space and time for imaging and focusing in complex media, Nat. Photonics 6 (2012) 283–292.
[14] J. Fade, S. Panigrahi, A. Carré, L. Frein, C. Hamel, F. Bretenaker, H. Ramachandran, M. Alouini, Long-range polarimetric imaging through fog, Appl. Opt. 53 (2014) 3854–3865.
[15] S.P. Duran, J.M. Porter, T.E. Parker, Ballistic imaging of diesel sprays using a picosecond laser: characterization and demonstration, Appl. Opt. 54 (2015) 1743–1749.
[16] J.B. Schmidt, Z.D. Schaefer, T.R. Meyer, S. Roy, S.A. Danczyk, J.R. Gord, Ultrafast time-gated ballistic-photon imaging and shadowgraphy in optically dense rocket sprays, Appl. Optics 48 (2009) B137–B144.
[17] L. Wang, P.P. Ho, C. Liu, G. Zhang, R.R. Alfano, Ballistic 2-D imaging through scattering walls using an ultrafast optical Kerr gate, Science 253 (1991) 769–771.
[18] H.L. Xu, S.L. Chin, Femtosecond laser filamentation for atmospheric sensing, Sensors 11 (2011) 32–53.
[19] W. Chu, H.L. Li, J.L. Ni, B. Zeng, J.P. Yao, H.S. Zhang, G.H. Li, H.L. Xu, Y. Cheng, Lasing action induced by femtosecond laser filamentation in ethanol flame for combustion diagnosis, Appl. Phys. Lett. 104 (2014) 091106.

[20] H. Purwar, S. Idlahcen, C. Rozé, D. Sedarsky, J.B. Blaisot, Collinear, two-color optical Kerr effect shutter for ultrafast time-resolved imaging, Opt. Express 22 (2014) 15778–15790.
[21] F.X. D'Abzac, M. Kervella, L. Hespel, T. Dartigalongue, Experimental and numerical analysis of ballistic and scattered light using femtosecond optical Kerr gating: a way for the characterization of strongly scattering media, Opt. Express 20 (2012) 9604–9615.
[22] W. Tan, Z. Zhou, A. Lin, J. Si, P. Zhan, B. Wu, X. Hou, High contrast ballistic imaging using femtosecond optical Kerr gate of tellurite glass, Opt. Express 21 (2013) 7740–7747.
[23] H. Zhang, H. Liu, J. Si, W. Yi, F. Chen, X. Hou, Low threshold power density for the generation of frequency up-converted pulses in bismuth glass by two crossing chirped femtosecond pulses, Opt. Express 19 (2011) 12039–12044.
[24] H. Liu, H. Zhang, J. Si, L. Yan, F. Chen, X. Hou, Elimination of the coherent artifact in a pump- probe experiment by directly detecting the background-free diffraction signal, Chin. Phys. Lett. 28 (2011) 0866021–0866024.
[25] Z. Falgout, M. Rahm, D. Sedarsky, M. Linne, Gas/fuel interfaces under high pressures and temperatures, Fuel 168 (2016) 14–21.
[26] S. Idlahcen, L. Méès, C. Rozé, et al., Time gate, optical layout, and wavelength effects on ballistic imaging, J. Opt. Soc. Am. A 26 (2009) 1995–2004.
[27] L. Gundlach, P. Piotrowiak, Femtosecond Kerr-gated wide-field fluorescence microscopy, Opt. Lett. 33 (2008) 992–994.
[28] L. Yan, J. Yue, J. Si, X. Hou, Influence of self-diffraction effect on femtosecond pump-probe optical Kerr measurements, Opt. Express 16 (2008) 12069–12074.
[29] B.J. Rudresha, B.R. Bhat, D. Ramarkrishna, J.K. Anthony, H.W. Lee, F. Rotermund, Nonlinear optical study of palladium Schiff base complex using femtosecond differential optical Kerr gate and Z-scan techniques, Opt. Laser Technol. 44 (2012) 1180–1183.
[30] F. Mathieu, M.A. Reddemann, J. Palmer, R. Kneer, Time-gated ballistic imaging using a large aperture switching beam, Opt. Express 22 (2014) 7058–7074.
[31] K. Mantel, N. Lindlein, J. Schwider, Simultaneous characterization of the quality and orientation of cylindrical lens surfaces, Appl. Opt. 44 (2005) 2970–2977.